ISSN 1054-660X, Laser Physics, 2012, Vol. 22, No. 3, pp. 554–558.
© Pleiades Publishing, Ltd., 2012.
Original Text © Astro, Ltd., 2012.

Power and Spectra Polarization of Large-Aperture Rectangular-Shaped Vertical-Cavity Top-Emitting Lasers[1]

W. Wang[a, b], Y. Q. Ning[a, *], J. L. Zhang[a], L. Qin[a], Y. G. Zeng[a], Y. Liu[a], C. Z. Tong[a], and L. J. Wang[a]

[a] *Key State Laboratory of Luminescence and Their Applications, Changchun Institute of Optics, Fine Mechanics and Physics, Chinese Academy of Sciences, Changchun, 130033 China*

[b] *Graduate School of Chinese Academy of Sciences, Beijing, 100039 China*

*e-mail: ningyq@ciomp.ac.cn

Received October 14, 2011; in final form, October 15, 2011; published online February 6, 2012

Abstract—980-nm large-aperture top-emitting vertical-cavity surface-emitting lasers (VCSELs) were investigated through introducing the rectangular post. Both H-polarization (horizontal) and V-polarization (vertical) coexisted in the rectangular-shaped large-aperture VCSELs. Under the entire range of operation current, H-polarization dominated over V-polarization which was parallel to the shorter side of the rectangular output aperture. It was found that spectrum blue-shift of H-polarization light occurred with respect to V-polarization light at three different aspect ratios, and this can be explained by the dependence of longitudinal propagation constant on the aspect length. The rectangular post structure was found to be effective for polarization stabilization in broad-area VCSELs without serious degradation of light output characteristics.

DOI: 10.1134/S1054660X1203022X

1. INTRODUCTION

In the last few decades there has been an increasing interest in the vertical-cavity surface-emitting lasers (VCSELs) due to their attractive features, particularly the polarization property which is one of the most crucial factors among them. Unlike conventional edge emitting lasers, where the large gain difference between TE and TM modes and the anisotropic structure geometry determine the output polarization in a natural way, cylindrically symmetry VCSELs are inclined to polarization instabilities [1, 2]. That is a limiting factor for polarization-sensitive applications, such as optical communication, optical information processing, and magneto-optic memories. And polarization switching is dependent on the variation of the external conditions such as the temperature and the drive current [3, 4]. Thus extensive attempts have been made to stabilize the polarization states of VCSELs by using fine metal-interlaced gratings [5], external optical feedback [6], electro-optic birefringence [7], photonic crystal [8], and C-shaped nanoaperture [9].

However, the methods mentioned above are all applied into small-aperture VCSELs with stable output polarization. In small-aperture devices the polarization is closely related to the material anisotropies, but the polarization investigation of large-aperture VCSELs is limited by the appearance of much more high order transverse modes being a manifestation of self-organization in nonequilibrium systems due to large sizes and current crowding [10, 11]. The beam divergence was improved by surface plasmon modulated nano-aperture in small-aperture device [12]. Most VCSEL researchers anticipated that polarization could be stabilized by introducing anisotropy in the VCSEL design [13], and we have used the rectangular post in bottom-emitting VCSELs [14], but this approach has not successfully applied in large-aperture top-emitting VCSELs.

In this paper, we described our method through the introduction of rectangular post in large-aperture top-emitting VCSELs. In the following, the light output characteristics were presented in large-aperture rectangular-shaped top-emitting VCSELs. Power polarizations were demonstrated with different output apertures under the operation current. Spectra polarizations of rectangular-shaped top-emitting VCSELs were experimentally presented and some discussions were also carried out.

2. FABRICATION

A schematic structure of 980-nm large-aperture rectangular-shaped top-emitting VCSEL was shown in Fig. 1. The wafer of device was grown by metal organic chemical vapor deposition (MOCVD) with good uniformity on an N-type ⟨001⟩-GaAs substrate misoriented 2° toward ⟨110⟩. The VCSEL had a three-quantum-well $In_{0.17}Ga_{0.83}As$ active layer, which was sandwiched by a 23 pairs P-type $Al_{0.9}Ga_{0.1}As/Al_{0.12}Ga_{0.88}As$ distributed Bragg reflector (DBR) mirror doping carbon and a 38 pairs N-type $Al_{0.9}Ga_{0.1}As/Al_{0.12}Ga_{0.88}As$ DBR mirror doping silicon. To form the rectangular post mesa structure, photolithography and wet etching were used for patterning the posts from the top layer to the high Al layer, and making rectangular pattern resist masks [15]. The oxi-

[1] The article is published in the original.

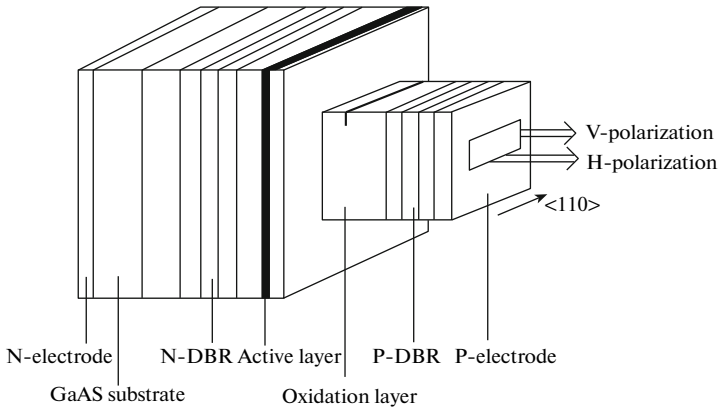

Fig. 1. Three-dimensional schematic structure of 980 nm large-aperture rectangular-shaped top-emitting VCSEL.

dation layer was inserted to reduce the sidewall loss and current crowding [16]. Since it has been experimentally demonstrated that practical VCSELs emit linearly light with the preference of the polarization direction along the $\langle 110 \rangle$ or $\langle 1\bar{1}0 \rangle$ crystallographic axes [17], the longer side of rectangular output aperture is aligned to $\langle 110 \rangle$ crystal orientation, as depicted in Fig. 1. On the top of P-DBR mirror, the output apertures were obtained by etching Ti/Au layer which was deposited for forming ohmic P-electrode. The current confinement was attained mainly by the output aperture, because the output aperture was much smaller than the oxidation window. Finally, AuGeNi/Au layers were deposited on the GaAs substrate for making the N-electrode contact. The output light was emitted from the top of the rectangular mesa through the P-DBR mirror. In our experiment, large-aperture VCSELs were fabricated with three kinds of output apertures such as 50×150, 50×200, and 50×250 μm^2.

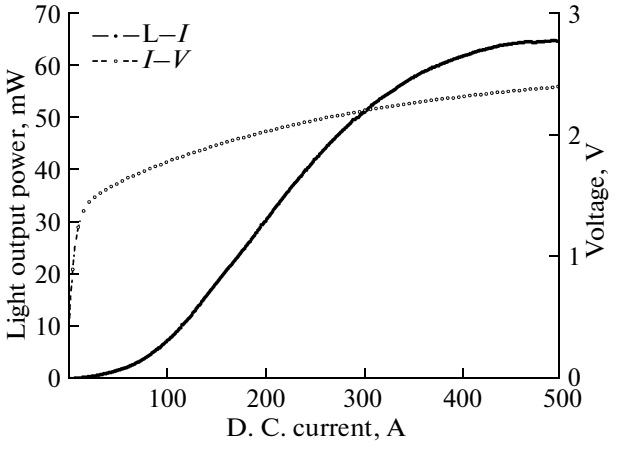

Fig. 2. Light output power-current-voltage (L–*I*–*V*) characteristics of 980-nm rectangular-shaped VCSELs with 50×200 μm^2 output aperture.

3. RESULTS AND DISCUSSION

In the experiment, the measurements of VCSELs were performed under continuous wave (cw) operation at room temperature (RT) and direct current was injected from the electrodes into the active region. As can be signified in Fig. 2, the light power-current-voltage (L–*I*–*V*) characteristics of 980-nm large-aperture rectangular-shaped vertical-cavity top-emitting lasers were demonstrated with output aperture 50×200 μm^2. The dashed line was *I*–*V* curve and the solid line was L–*I* line describing the total optical power property. In this figure, it was obviously indicated that laser power up to 65 mW can be emitted from the rectangular-shaped top-emitting VCSELs while the injected current reached 500 mA. Correspondingly, the induced threshold current (about 50 mA) was the drawback offered by large-aperture VCSELs and the threshold current density was 500 A/cm^2. The differential resistance was 1.15 Ω. The output performance was not degenerate in rectangular-shaped VCSELs. Aiming at improving the output power of VCSEL, multi-ring-shaped-aperture structure was recently reported to achieve high power three times than single large aperture [18]. And low beam divergence was obtained in colliding-pulse mode-locked lasers [19].

In order to study the polarization properties of VCSELs, polarization beam splitter (PBS) was used during the measurement. In this paper, the emitting laser parallel to the longer side and the shorter side were defined as H-polarization (horizontal) light and V-polarization (vertical) light, respectively. It was commonly believed that much more complicated modes would take place when the transverse geometry sizes got broad in VCSELs, and they could be coupled with each other for linear fitting. It was reported that only three supermodes appeared at most in hybrid

point/ring-defect photonic crystal VCSEL [20]. Therefore, linear polarizations of optical beam would be taken into account such as horizontal and vertical polarizations, instead of every single mode. Single-mode holey was reported to narrow the beam divergence in small-aperture VCSEL [21], and coherence functions of electrical and optical noise in single-mode packaged VCSEL was also reported [22].

As was indicated in Fig. 3, power polarization of large-aperture top-emitting VCSELs were presented with three different output apertures: (a) 50 × 150; (b) 50 × 200; and (c) 50 × 250 μm^2, there was a distinct region above the lasing threshold where the VCSEL emission was linearly polarized. Apparently, both H-polarization and V-polarization demonstrated coexistence over the entire range of operation current. The main origin of the polarization stabilization was considered to be the gain saturation, and cross-effect between the two different oscillation directions was produced [23]. As a result of the spatial symmetry of current injection structure, polarization dual-stabilization was achieved by cross gain saturation between the two polarization directions of rectangular output window where the transverse sizes became wider. In this figure, H-polarization dominated over V-polarization during the operation current in power polarization curves. Furthermore, concerning the relationship between polarization ratio and aspect ratio of output aperture, the most outstanding polarization ratio (about 2) between H-polarization and V-polarization was given while the aspect ratio was 1:3 (50:150), and this could be appropriate for polarization-sensitive applications. When the shorter side of rectangular aperture was fixed to 50 μm, the polarization ratio between H-polarization and V-polarization became smaller and smaller at the same injected current as the longer side was enhanced from 150 to 250 μm in 50 μm increments.

Besides output power, optical spectra polarization were checked out in the following, as manifested in Fig. 4. As was shown in Fig. 4, optical spectrums of H-polarization and V-polarization were demonstrated above lasing threshold with (a) 50 × 150, (b) 50 × 200 , and (c) 50 × 250 μm^2. It was found that spectrum blue-shift of H-polarization light occurred with respect to V-polarization light at three different aspect ratios. The spectral selection method was proposed based on weak coupling between a tilted short Fabry–Perot interferometer and a semiconductor optical amplifier [24]. The spectra difference for horizontal and vertical polarizations can be mainly expressed by centre wavelength shift. This phenomenon can be explained by symmetric three layer waveguide model. Assuming the core layer was the material of output aperture, GaAs, and the cladding layer was the air region. For one direction of the in-plane structure, the core layer and the cladding layer can form one-dimensional symmetric three layer waveguide model. The eigenvalue function of transverse propagation constant can be expressed as:

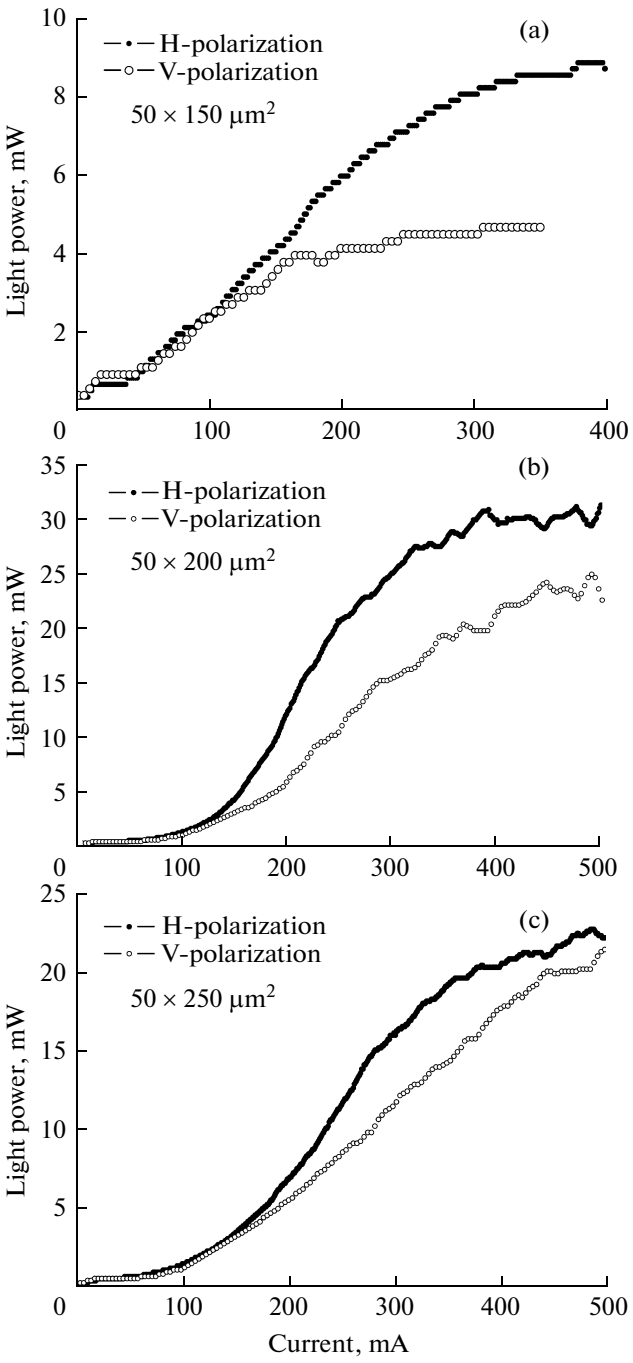

Fig. 3. Power polarization of large-aperture top-emitting VCSELs with three different output apertures: (a) 50 × 150; (b) 50 × 200; and (c) 50 × 250 μm^2.

$$qd = 2\arctan\left(\frac{\sqrt{k_0^2(n_1^2 - n_0^2) - q^2}}{q}\right) + m\pi, \quad (1)$$

$$m = 0, 1, 2, \ldots,$$

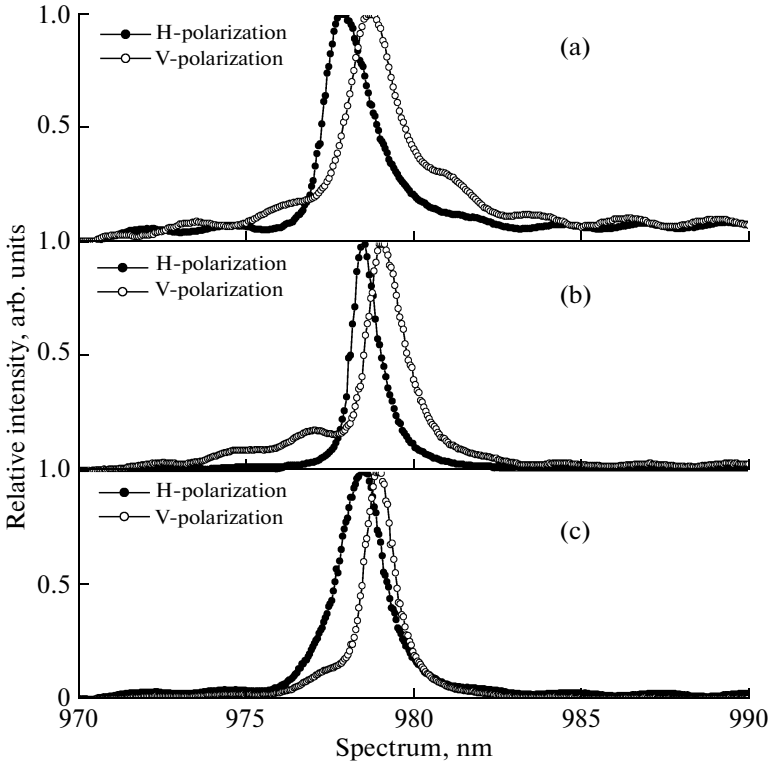

Fig. 4. Optical spectrum of H-polarization and V-polarization for VCSELs with three output apertures: (a) 50 × 150; (b) 50 × 200; and (c) 50 × 250 μm^2.

where q was the transverse propagation constant, d was the length of one side for the rectangular output aperture, n_1 was the refractive index of the core layer, n_0 was the refractive index of the cladding layer, and k_0 was the wave number for the lasing wavelength. For simplification, only $m = 0$ was considered. The dependence of the transverse propagation constant on the d value was displayed in Fig. 5. The wave number can be written as:

$$k_0 = \frac{2\pi}{\lambda_0}, \tag{2}$$

where λ_0 was the lasing wavelength, here $\lambda_0 = 980$ nm. The longitudinal propagation constant of the emitting laser can be described by:

$$\beta = \sqrt{k_0^2 n_1^2 - q^2}. \tag{3}$$

For H-polarization light and V-polarization light from the same output aperture, the longitudinal propagation constant of each polarization can be written:

$$\beta = n_{\text{eff}} \frac{2\pi}{\lambda}, \tag{4}$$

where n_{eff} was the effective refractive index of the output aperture, λ was the corresponding wavelength for H-polarization and V-polarization. For the rectangular output aperture, $d_H > d_V$. Combining Eqs. (1)–(4), it can be concluded that $\lambda_H < \lambda_V$. Therefore, blue-shift of H-polarization light happened with respect to V-polarization which was aligned to the shorted side of the output aperture.

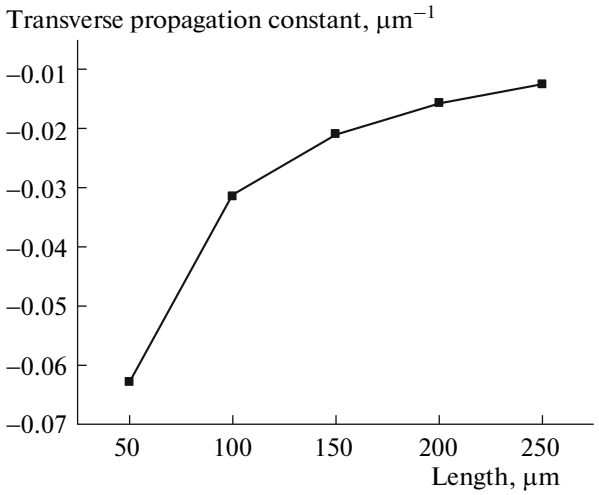

Fig. 5. The dependence of transverse propagation constant on the length of one side for the rectangular output aperture.

4. CONCLUSIONS

In summary, large-aperture 980-nm vertical-cavity top-emitting lasers were fabricated and investigated through the introduction of rectangular post. Both H-polarization and V-polarization demonstrated coexistence over the entire range of operation current, and H-polarization dominated over V-polarization which was parallel to the shorter side of the rectangular output aperture. It was found that spectrum blue-shift of H-polarization light occurred with respect to V-polarization light at three different aspect ratios. It can be explained by the symmetric three layer waveguide model proposed in the paper. The rectangular post structure was found to be effective for polarization stabilization in large-aperture VCSELs without serious degradation of light output characteristics. These results would make it possible to utilize large-aperture VCSELs arrays with polarization-sensitive optical element, and will thereby significantly advance VCSEL applications.

ACKNOWLEDGMENTS

This research work was supported by the National Science Foundation grant (60636020, 60706007, 10974012, 60876036, 90923037, 11074247, 61006054).

REFERENCES

1. D. Burak, J. V. Moloney, and R. Binder, IEEE J. Quantum Electron. **36**, 956 (2000).
2. J. Martin-Regalado, J. L. A. Chilla, J. J. Rocca, and P. Brusenbach, Appl. Phys. Lett. **70**, 3350 (1997).
3. K. Hasebe, Y. Onishi, and F. Koyama, Electron. Commun. Jpn. **90**, 41 (2007).
4. Y. Sato, K. Furuta, T. Katayama, and H. Kawaguchi, IEEE Photon. Technol. Lett. **20**, 1446 (2008).
5. Jung-Hoon Ser, Young-Gu Ju, Jae-Heon Shin, and Y. H. Lee, Appl. Phys. Lett. **66**, 2769 (1995).
6. T. H. Russell and T. D. Milster, Appl. Phys. Lett. **70**, 2520 (1997).
7. M. S. Park, B. T. Ahn, Byueng-Su Yoo, et al., Appl. Phys. Lett. **76**, 813 (2000).
8. Dae-Sung Song, Yong-Jae Lee, Han-Woo Choi, and Yong-Hee Lee, Appl. Phys. Lett. **82**, 3182 (2003).
9. Z. L. Rao, J. A. Matto, L. Hesselink, and J. S. Harris, Appl. Phys. Lett. **90**, 191110 (2007).
10. I. V. Babushkin, M. Schulz-Ruhtenberg, N. A. Loiko, et al., Phys. Rev. Lett. **100**, 213901 (2008).
11. X. Hachair, G. Tissoni, H. Thienpont, and K. Panajotov, Phys. Rev., Ser. A **79**, 011801 (R) (2009).
12. J. Gao, G. Song, Q. Gan, et al., Laser Phys. Lett. **4**, 234 (2007).
13. T. Yoshikawa, T. Kawakami, H. Saito, et al., IEEE J. Quantum Electro. **34**, 1009 (1998).
14. W. Wang, Y. Q. Ning, Z. H. Tian, et al., Opt. Commun. **284**, 1335 (2011).
15. T. Yoshikawa, H. Kosaka, K. Kurihara, et al., Appl. Phys. Lett. **66**, 908 (1995).
16. M. S. Alias, S. Shaari, and S. M. Mitani, Laser Phys. **20**, 806 (2010).
17. G. Verschaffelt, W. van der Vleuten, M. Creusen, et al., IEEE Photon. Technol. Lett. **12**, 945 (2000).
18. Y. Q. Hao, C. Y. Shang, Y. Feng, et al., Laser Phys. **21**, 376 (2011).
19. L. P. Hou, M. Haji, C. Li, et al., Laser Phys. Lett. **8**, 535 (2011).
20. A. J. Liu, W. Chen, H. W. Qu, et al., Laser Phys. **21**, 379 (2011).
21. A. J. Liu, W. Chen, H. W. Qu, et al., Laser Phys. Lett. **7**, 213 (2010).
22. F. Principato, G. Ferrante, and F. Marin, Laser Phys. Lett. **4**, 204 (2007).
23. H. Kawaguchi, Opto-Electronics Rev. **17**, 265 (2009).
24. A. A. Moiseev, G. V. Gelikonov, E. A. Mashcovitch, and V. M. Gelikonov, Laser Phys. Lett. **7**, 505 (2010).